

A WEB OF CONFOCAL PARABOLAS IN A GRID OF HEXAGONS

PETER MOSES AND DAN REZNIK

ABSTRACT. If one erects regular hexagons upon the sides of a triangle T , several surprising properties emerge, including: (i) the triangles which flank said hexagons have an isodynamic point common with T , (ii) the construction can be extended iteratively, forming an infinite grid of regular hexagons and flank triangles, (iii) a web of confocal parabolas with only three distinct foci interweaves the vertices of hexagons in the grid. Finally, (iv) said foci are the vertices of an equilateral triangle.

Keywords hexagon, flank, map, isodynamic, parabola, confocal.

MSC 51M04 and 51N20 and 51N35 and 68T20

1. INTRODUCTION

Napoleon's theorem is illustrated in [Figure 1](#)(left): the centroids of the 3 equilaterals erected upon the sides of a reference triangle $T = ABC$ are vertices of an equilateral known as the “outer” Napoleon triangle [\[15\]](#). A related construction due to Lamoen appears in [Figure 1](#)(right), whereby squares are erected upon the sides of T and triangles which “flank” said squares are defined [\[12\]](#).

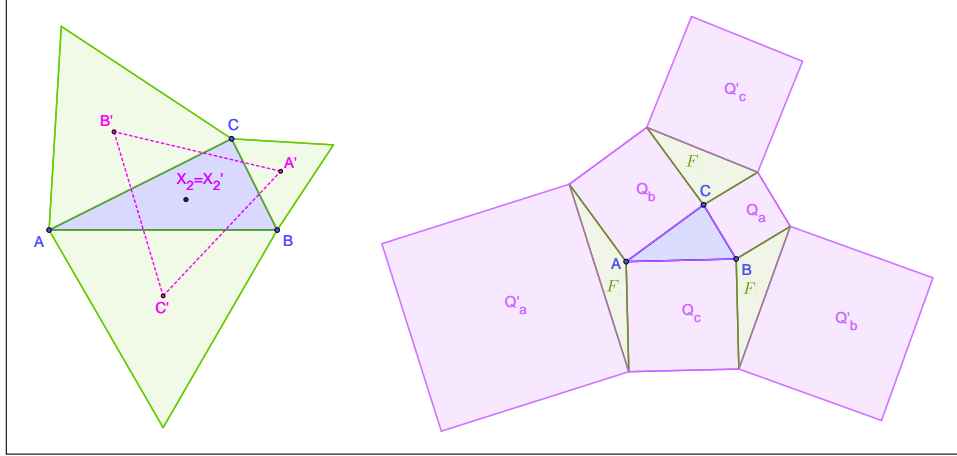


FIGURE 1. **Left:** Napoleon's theorem affirms that a triangle $\mathcal{T}' = A'B'C'$ (dashed magenta) whose vertices are the centroids of 3 equilaterals (green) erected upon the sides of a triangle $\mathcal{T} = ABC$ (blue) is itself equilateral. Furthermore, its centroid coincides with the barycenter X_2 of \mathcal{T} [\[15, Napoleon's Thm\]](#). **Right:** Lamoen [\[12\]](#) has studied properties of “flank” triangles F defined between neighboring squares Q_a, Q_b, Q_c erected upon the sides of a $\mathcal{T} = ABC$, as well as those of additional squares Q'_a, Q'_b, Q'_c erected upon the flanks.

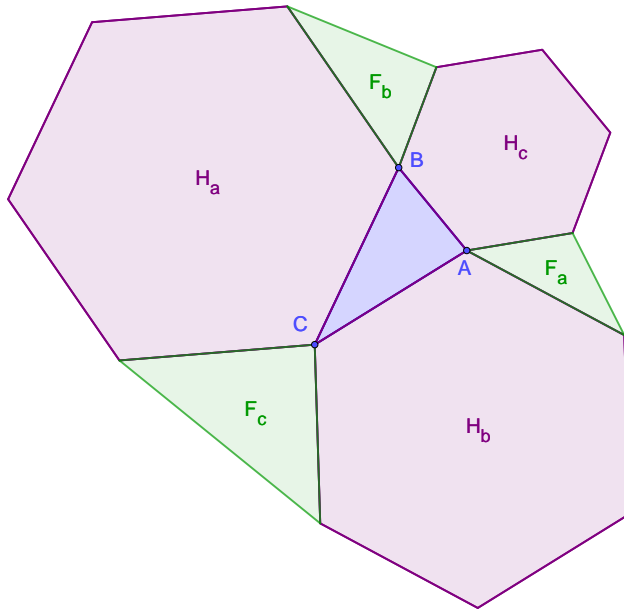


FIGURE 2. Given a reference triangle $\mathcal{T} = ABC$, erect three regular hexagons $\mathcal{H}_a, \mathcal{H}_b, \mathcal{H}_c$ on its sides; these define three flank triangles with a vertex at A, B , or C (respectively), and two others which are proximal vertices of erected hexagons sharing A, B , or C , respectively.

We borrow from those ideas and study a construction whereby regular *hexagons* $\mathcal{H}_a, \mathcal{H}_b, \mathcal{H}_c$ are erected upon the sides of \mathcal{T} , with 3 “flank” triangles F_a, F_b, F_c defined between them, see Figure 2. As it turns out, many surprising properties emerge, listed below.

Summary of the Results.

- The second isodynamic points [15] of \mathcal{T} and the flanks are common;
- A contiguous, infinite grid of regular hexagons can be constructed, see Figure 8; all flanks in the grid have a common second isodynamic point and conserve a special quantity;
- Sequences of hexagon vertices are crisscrossed by a web of confocal parabolas with only 3 distinct foci;
- Their foci and directrix intersections are vertices of 2 new equilateral triangles;
- Phenomena are described when the reference triangle in Figure 2 are triangles in two special Poncelet triangle families.

Related Work. In [3, 12] properties of “flank” triangles located between squares and/or rectangles erected on a triangle’s sides are studied. Works [4, 9] study triangles centers (taken as triples or not) analogues of the intouch and/or extouch triangles erected upon each side of a reference triangle. In [6, 7, 14, 2] a construction related to Napoleon’s theorem is described which associates to a generic triangle a regular hexagon.

Article Structure. In Section 2 we describe properties of the trio of flank triangles. In Section 3 we fix a central regular hexagon and consider properties of 6 “satellite”

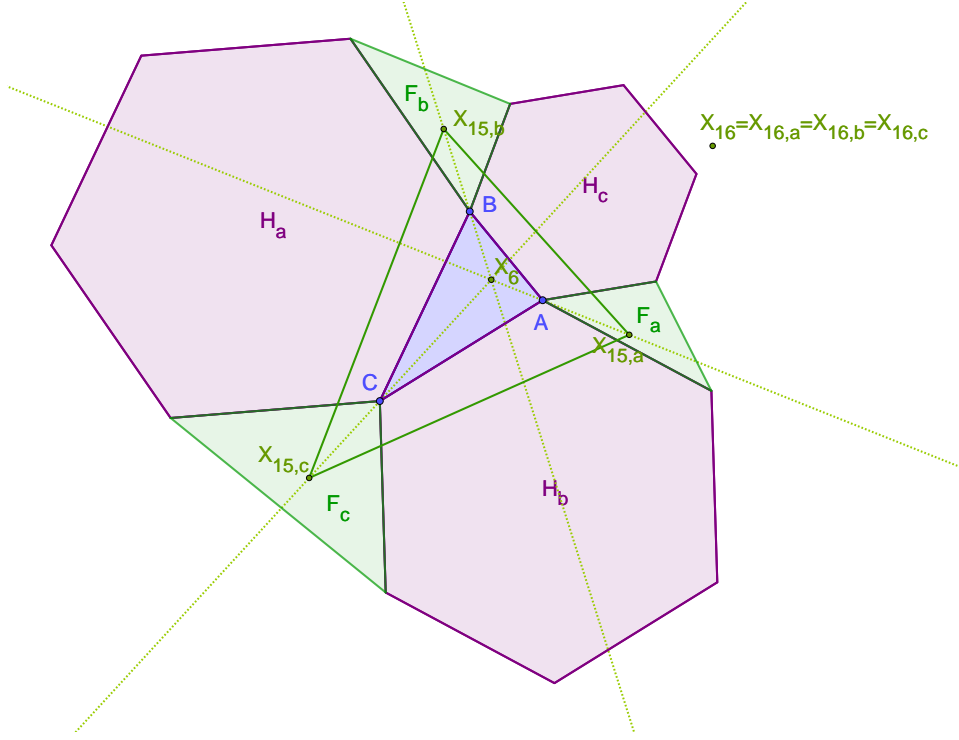


FIGURE 3. (i) the triangle formed by the 1st isodynamic points $X_{15,a}$, $X_{15,b}$, $X_{15,c}$ of the 3 flank triangles is perspective with $\mathcal{T} = ABC$ at the latter's X_6 ; (ii) the 2nd isodynamic point of \mathcal{T} and the 3 flank triangles are common (upper right).

triangles built around it, and this implies a contiguous grid can be iteratively built. In Section 4 we show said grid is interwoven by three groups of confocal parabolas. In Section 5 we show two examples of grids controlled by Poncelet poristic triangles. Section 6 provides a table of videos illustrating some results as well as a list of open questions. In Appendix A we provide computer-usable expressions for some objects described in Section 4.

2. HEXAGONAL FLANKS

Adhering to Kimberling's X_k notation for triangle centers [11], recall a triangle's *isodynamic points* X_{15} and X_{16} are the limiting points of a pencil¹ of circles containing a triangle's circumcircle and the Brocard circle [15, Isodynamic Points].

Referring to Figure 3:

Proposition 1. *The triangle with vertices on the X_{15} -of-flanks is perspective with \mathcal{T} at the latter's symmedian point X_6 .*

Proof. A straightforward derivation for the barycentrics of X_{15} of the A -flank yields $(a^2 - 3b^2 - 3c^2, b^2, c^2)$, and those of the B - and C -flanks can be obtained cyclically. Recall the barycentrics of X_6 are (a^2, b^2, c^2) , so the result follows. \square

¹This pencil is known as the *Schoutte pencil* [10].

Proposition 2. *The 2nd isodynamic points X_{16} of the three flank triangles coincide with that of \mathcal{T} .*

The following proof sketch was kindly contributed by D. Grinberg [8]:

Proof. Let two triangles $\mathcal{T} = ABC$ and $\mathcal{T}' = A'B'C'$ be called “30-twins around B” iff $B = B'$ and $\angle BAA' = \angle AA'B = 30^\circ$ and $\angle BC'C = \angle CC'B = 30^\circ$ (angles are in degrees and are directed angles mod 180°). In other words, this is the relation between \mathcal{T} its flank triangle at B. It is a symmetric relation, up to relabeling ABC as CBA to get the correct orientation.

Let ABC and $A'BC'$ be two triangles that are 30-twins around B . Fix a nontrivial circle K around B , and let X, Z, X' and Z' be, respectively, the images of A, C, A' and C' under the inversion with respect to K . It can be shown that it follows that triangles XBZ and $X'BZ'$ are again 30-twins around B .

The same inversion takes X_{16} of ABC to the third vertex of an equilateral triangle erected inwardly on the side XZ of triangle XBZ . The proof is an angle chase, using the fact that X_{16} is the unique point of a triangle which sees the three vertices at 120° angles [15, Isodynamic point]. The same applies for X_{15} and an equilateral triangle erected outwardly. Likewise for triangle $A'BC'$ and $X'Z'$.

Thus, it remains to be shown that the third vertex of an equilateral triangle erected inwardly on the side XZ of triangle XBZ is identical to the third vertex of an equilateral triangle erected inwardly on side $X'Z'$ of triangle $X'BZ'$. This is easy to prove using complex numbers: $w^2 + w + 1 = 0$ with $w = e^{2\pi i/3}$. \square

2.1. Zero-Area Flanks. Consider a family of triangles ABC where A, B are fixed and C is free. Let F_c denote the flank triangle between the regular hexagons erected upon AC and CB . As shown in Figure 4:

Observation 1. *F_c will be zero-area if C subtends a 120° angle, i.e., it lies on a circular arc centered on the centroid O of an equilateral erected upon AB and with radius $|OA|$.*

Consider the construction for the two flank triangles F_1 and F_2 shown in Figure 5, namely, departing from $\mathcal{T} = ABC$, erect regular hexagons \mathcal{H}_1 and \mathcal{H}_2 on sides AC and BA , respectively. Consider the a first flank triangle F_1 between \mathcal{H}_1 and \mathcal{H}_2 . As shown in the figure, erect a third regular hexagon \mathcal{H}_3 on the unused side of F_1 , and let a second flank triangle F_2 sit between \mathcal{H}_2 and \mathcal{H}_3 . While holding B and C fixed, there are positions for A such that F_2 has positive, zero, or negative signed area. Referring to Figure 6:

Proposition 3. *F_2 will have positive (resp. negative) area if A is exterior (resp. interior) to the circumcircle \mathcal{C} of an equilateral triangle whose base is B and the midpoint of BC . In particular, the vertices of F_2 become collinear if A is on \mathcal{C} .*

3. SATELLITE TRIANGLES

Consider the construction shown in Figure 7: given a triangle $\mathcal{T} = ABC$, erect regular regular hexagons \mathcal{H}_0 and \mathcal{H}_1 on sides BC and AB . These define a first flank triangle F_1 . Continue adding hexagons $\mathcal{H}_2, \dots, \mathcal{H}_5$, defining with \mathcal{H}_0 new flank triangles F_2, \dots, F_5 . Let D (resp. E) be a vertex of F_5 which is common to \mathcal{H}_0 and \mathcal{H}_5 (resp. located on \mathcal{H}_5 and adjacent to D).

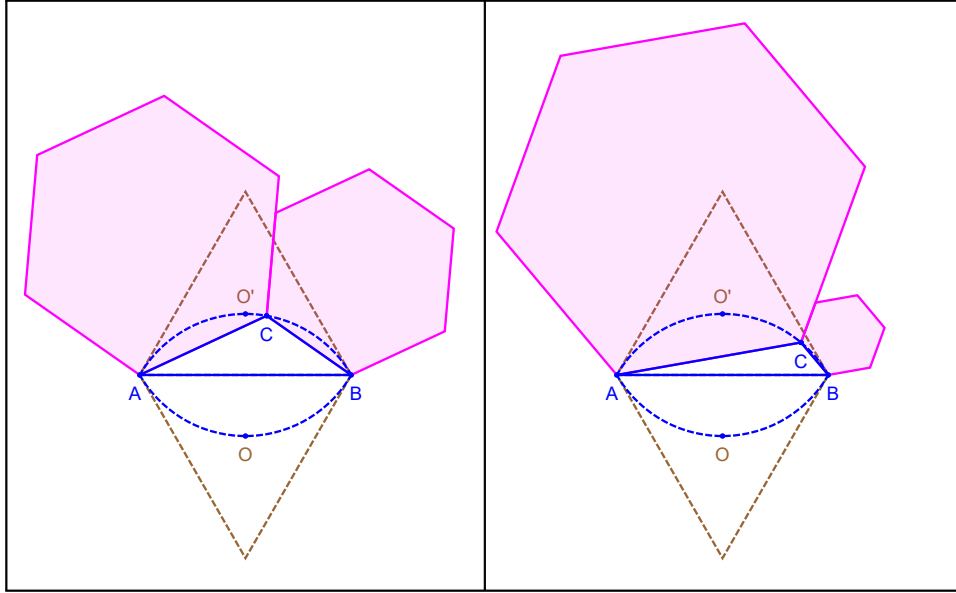


FIGURE 4. The locus of vertex C such that it subtends a 120° angle, i.e., the C -flank is degenerate, is a circular arc (dashed blue) such centered on O , the centroid of an equilateral (dashed brown) erected upon AB , and with radius $|OA|$ (a mirror arc corresponding to the top equilateral centered on O' is also shown). The left (resp. right) picture shows C in two distinct positions.

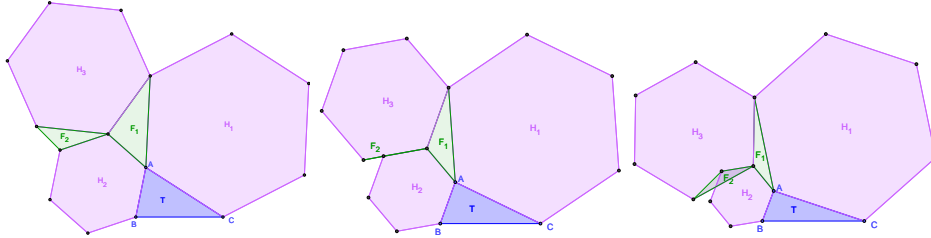


FIGURE 5. For certain positions of A (while keeping B and C stationary), flank triangle F_2 will be non-eversed (left), degenerate (middle), or eversed (right).

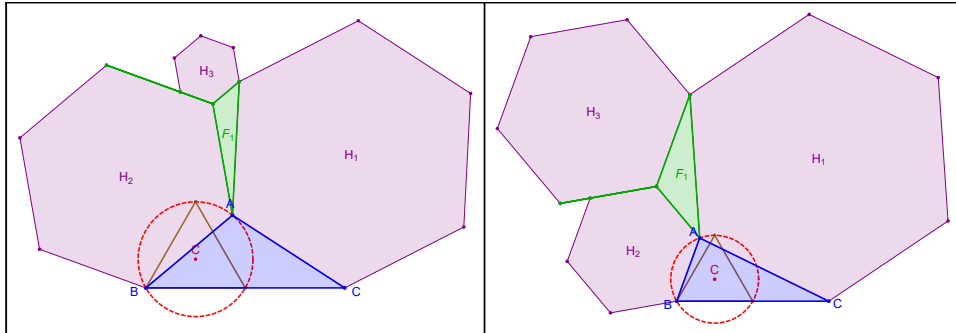


FIGURE 6. With B and C fixed, the locus of A such that the area of F_2 in Figure 5 is zero is the circumcircle (dashed red) of an equilateral (brown) with base on B and the midpoint of BC . Two positions of A are shown (left, right).

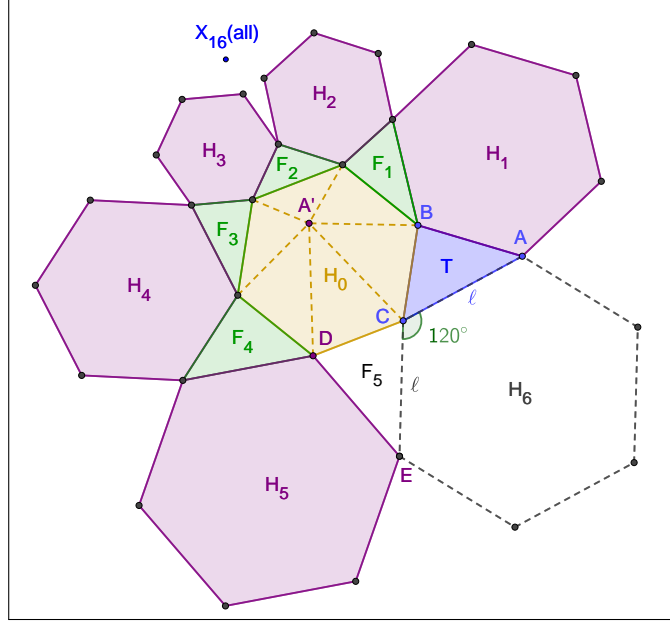


FIGURE 7. The grid “closure” property: departing from $\mathcal{T} = ABC$ add regular hexagons $\mathcal{H}_0, \dots, \mathcal{H}_5$ and flanks F_1, \dots, F_5 . The reflection of the apices of F_i about their based (sides of \mathcal{H}_i) is a common point A' . This implies the regular hexagon \mathcal{H}_6 erected on AC fits perfectly between \mathcal{H}_1 and \mathcal{H}_5 . The X_{16} common to \mathcal{T} and the five flanks is shown in the upper left of the picture.

Let A' be the reflection of A about BC . The following lemma was kindly contributed by A. Akopyan [1]:

Lemma 1. *The reflection of the apices of F_1, \dots, F_5 all coincide with A' .*

Still referring to Figure 7, let CE be the side of F_5 not on \mathcal{H}_0 nor on \mathcal{H}_5 . We can use Lemma 1 to show that:

Proposition 4. $|CE| = |AC|$ and $\angle ECA = (2\pi)/3$.

This implies that a sixth, regular hexagon \mathcal{H}_6 can be erected on AC and one of its vertices will snap perfectly against vertex E of \mathcal{H}_5 . Referring to Figure 8:

Corollary 1. *This construction can be extended ad infinitum, creating, modulo self-intersections, a locally-consistent contiguous grid.*

Since in this infinite grid one can isolate a central triangle and the three flanks around it (see Figure 2), you get the following propagation:

Corollary 2. *The second isodynamic points X_{16} of all flank triangles in any contiguous grid coincide in a single point.*

Consider the related construction in Figure 9: let \mathcal{H} denote a fixed regular hexagon with vertices Q_i , $i = 1, \dots, 6$. Given a point P , let Q_1Q_2P be a first “satellite” triangles F_1 . Create 5 new satellite triangles F_i as follows: Let F_i be the flank triangle obtained by erecting a regular hexagon on a side of F_{i-1} , $i = 2, \dots, 6$.

From Lemma 1 and Proposition 4, the reflected images of the flanks about their bases fill the interior of \mathcal{H} , therefore:

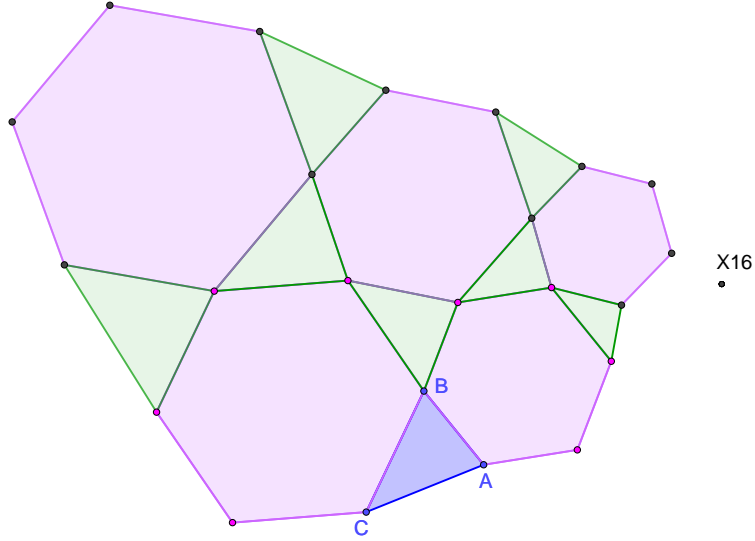


FIGURE 8. Departing from $\mathcal{T} = ABC$ a contiguous grid can be built by adding more triangles and regular hexagons as needed. The second isodynamic point X_{16} of all interstitial triangles is common with that of \mathcal{T} .

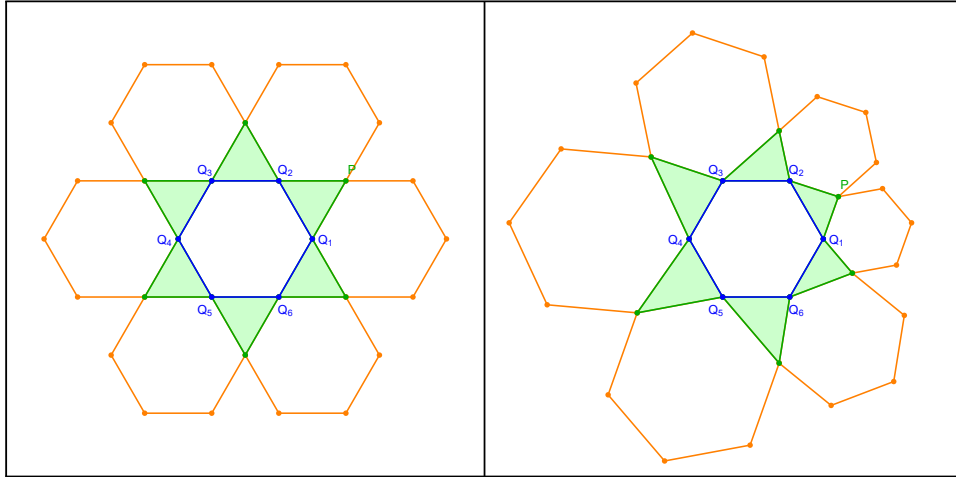


FIGURE 9. Given a fixed central hexagon \mathcal{H} with vertices $Q_i, i = 1, \dots, 6$, let 6 “satellite” flank triangles (green) be constructed around \mathcal{H} departing from a first triangle PQ_1Q_2 . The sum of areas of said 6 satellites is independent of P and equal to the area of \mathcal{H} . In the left (resp. right) P is positioned so the construction is regular (resp. irregular).

Corollary 3. *The sum of the areas of the 6 satellite triangles is independent of P and equal to the area of \mathcal{H} .*

Referring to Figure 10:

Proposition 5. *The apices of the 6 satellite triangles lie on a conic iff P lies on either line Q_3Q_2 or line Q_6Q_1 .*

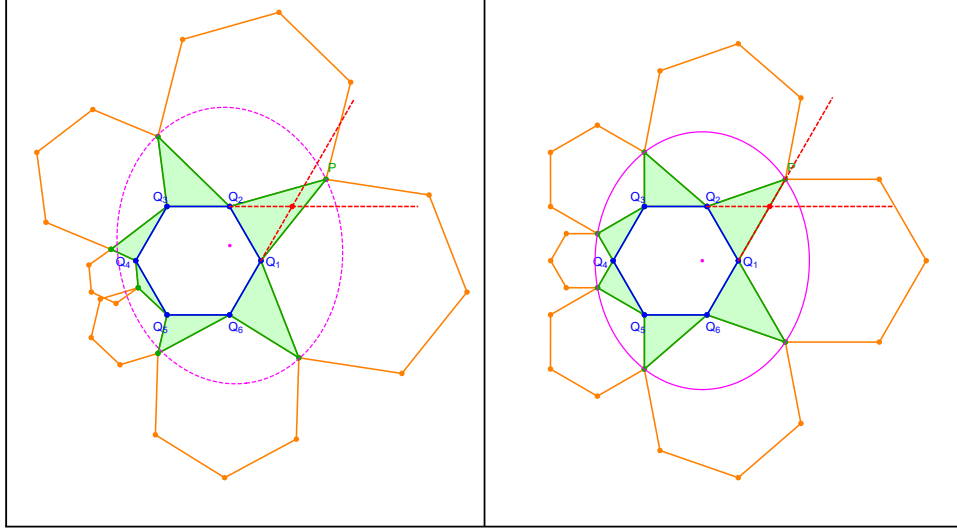


FIGURE 10. The apices of the 6 satellite triangles (green) around a fixed hexagon (blue) lie on a conic iff P is on either line Q_3Q_2 or line Q_6Q_1 . When P is at the intersection of said lines, the 6 apices are concyclic, as in Figure 9(left).

Referring to Figure 11, consider the 6 auxiliary regular hexagons erected successfully on the 6 satellite triangles parametrized by P . Let O denote the intersection of Q_3Q_2 and Q_6Q_1 .

Proposition 6. *The iso-curves of P such that the sum of the areas of the 6 satellite hexagons is constant are circles centered on O .*

3.1. Second-level satellites. Referring to Figure 12, consider the 6 satellite flanks F_i surrounding a central hexagon which are obtained as above by sequentially erecting 6 regular hexagons \mathcal{H}_i . Consider 6 “2nd-level” flanks F'_i nestled between the \mathcal{H}_i . Let \mathcal{H}'_k denote a hexagon whose vertices are the X_k of the F'_i .

Proposition 7. *For all X_k on the Euler line, \mathcal{H}'_k has invariant internal angles.*

We thank A. Akopyan for the following argument [1]:

Proof. This follows from the fact that their area is the sum of squares of distances from the reflected point A' to vertices Q_i of the central hexagon. \square

3.2. Properties of the Second Fermat Point. The second Fermat point X_{14} of a triangle is the isogonal conjugate of the second isodynamic point X_{16} [15, Fermat Points]. Let $\mathcal{H} = ABCDEF$ be a regular hexagon with centroid O , and let P be a point anywhere. Define six “inner” triangles $\mathcal{T}_1 = ABP$, $\mathcal{T}_2 = BCP$, ..., $\mathcal{T}_6 = FAP$. Referring to Figure 13(left): The second Fermat point X_{14} of a triangle is the isogonal conjugate of the second isodynamic point X_{16} [15, Fermat Points]. Let $\mathcal{H} = ABCDEF$ be a regular hexagon with centroid O , and let P be a point anywhere. $\mathcal{T}_1 = ABP$, $\mathcal{T}_2 = BCP$, ..., $\mathcal{T}_6 = FAP$. Referring to Figure 13(left):

Proposition 8. *The X_{14} of the \mathcal{T}_i will lie on PO .*

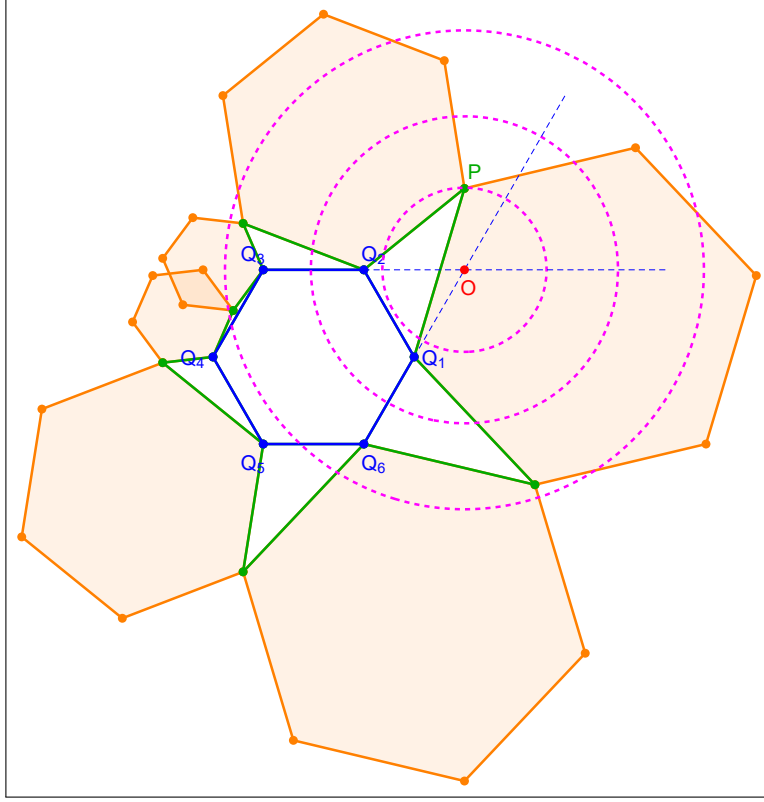


FIGURE 11. The iso-curves of P such that the sum of areas of the satellite hexagons is constant are circles (dashed magenta) centered on O , at the intersection of the two sides of \mathcal{H} adjacent to the base of PQ_1Q_2 .

Let \mathcal{T}'_i be the six triangles with (i) the base a side of \mathcal{H} , and (ii) the apex P'_i the reflection of P about said side. Assume in this case P is interior to \mathcal{H} . Referring to Figure 13(right):

Proposition 9. *The X_{14} of the \mathcal{T}'_i lie on a rectangular hyperbola (green) concentric with \mathcal{H} .*

4. A WEB OF CONFOCAL PARABOLAS

Referring to Figure 14, let, let $\mathcal{H}_i, \mathcal{H}_{i+1}$, etc., be adjacent hexagons in the grid sharing antipodal vertices U_i , such that one of the U_i is A . Let $\mathcal{H}'_i, \mathcal{H}'_{i+1}$, etc., be a second sequence of adjacent hexagons running along the same “grain” in the grid. The following was discovered by A. Akopyan [1]:

Proposition 10. *The sequence $\dots, U_{i-1}, A, U_{i+1}, \dots$ lies on a parabola which we call the A -parabola. Furthermore, similarly-constructed sequences of vertices along hexagons in the same diagonal direction lie on parabolas confocal with the A -parabola at f_a .*

Referring to Figure 15, a total of three groups of confocal parabolas can be constructed, along three “grains” in the grid. Let a, b, c denote the sides of $\mathcal{T} = ABC$, and S is Conway’s notation for twice the area of \mathcal{T} . Referring to Figure 16:

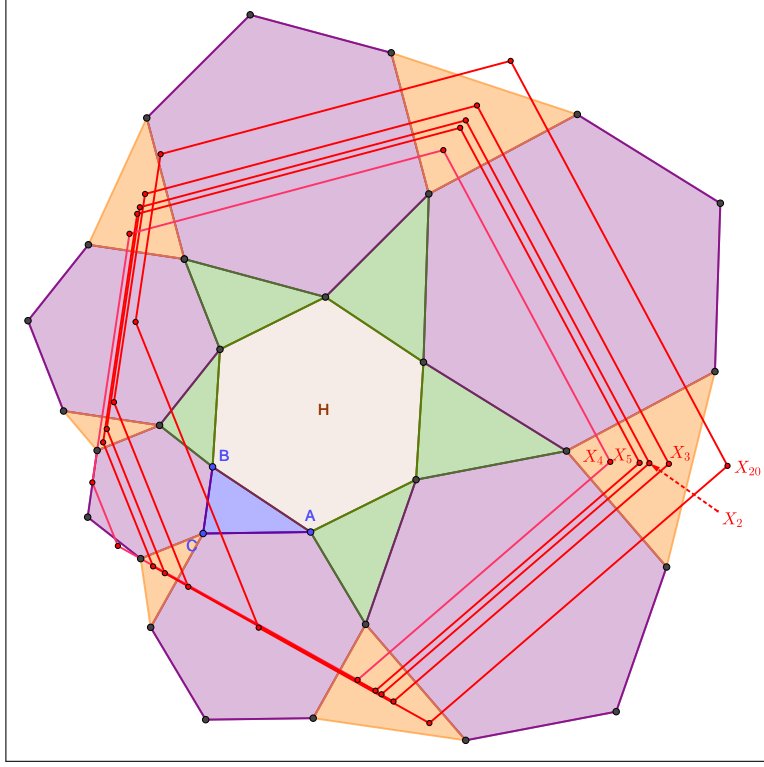


FIGURE 12. Shown are 5 hexagons \mathcal{H}'_i (red) whose vertices are the X_k of second-level satellites (yellow). If X_k is on the Euler line, the \mathcal{H}'_i have identical internal angles.

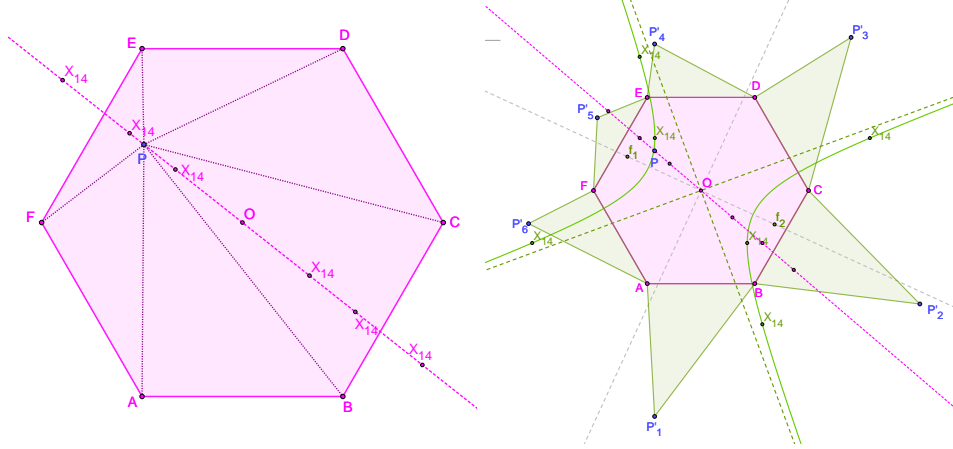


FIGURE 13. **Left:** Let $\mathcal{H} = ABCDEF$ be a regular hexagon, and P a point. The second Fermat points X_{14} of the “inner” triangles $\mathcal{T}_i \in \{ABP, BCP, \dots, FAP\}$ are collinear with P and the centroid O of \mathcal{H} . **Right:** Let \mathcal{T}'_i be triangles with base a side of \mathcal{H} , and apex P'_i the reflection of P about said side. The X_{14} of the \mathcal{T}'_i lie on a rectangular hyperbola (green) concentric with \mathcal{H} . Also shown is the (dotted magenta) line of the X_{14} of the inner triangles.

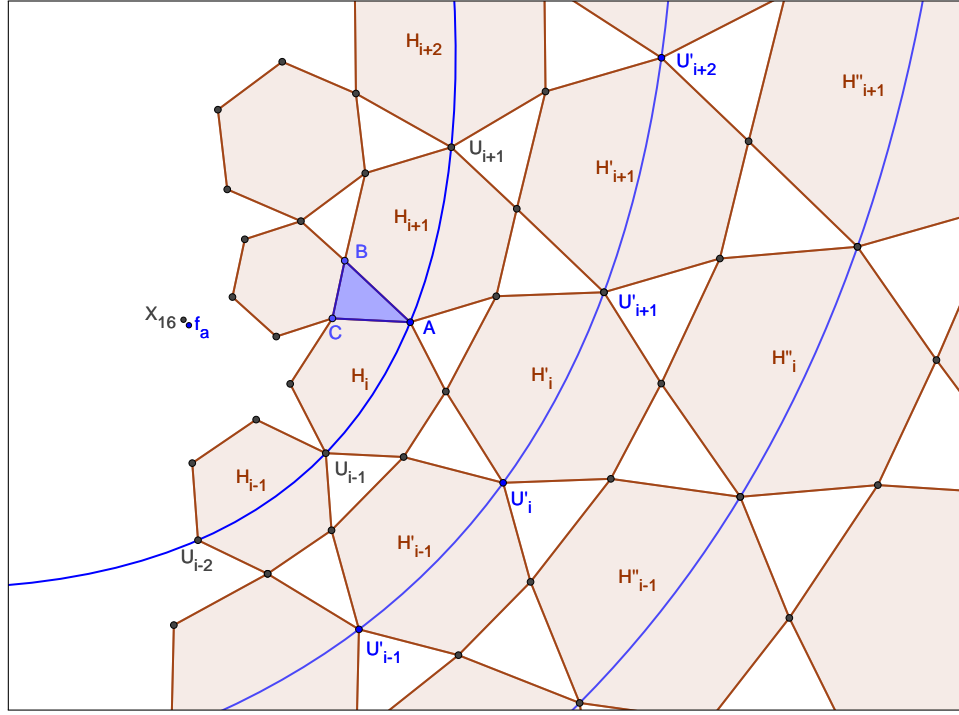


FIGURE 14. From hexagons $\mathcal{H}_{i-1}, \mathcal{H}_i$, etc., take antipodal vertices $U_{i-2}, U_{i-1}, A, U_{i+1}$. These lie on the A -parabola (blue), whose focus is f_a . Confocal parabolas pass through antipodal vertices along any other “row” of adjacent hexagons in the grid, e.g., $\mathcal{H}'_{i-1}, \mathcal{H}'_i, \mathcal{H}_{i+1}, \dots$

Theorem 1. *The foci of the three groups of confocal parabolas are vertices of an equilateral triangle with centroid at the X_{16} common to all flanks and \mathcal{T} . The barycentric coordinates of f_a are given by:*

$$f_a = \begin{bmatrix} \sqrt{3}(7a^2b^2 + 7a^2c^2 + 2b^2c^2 - 4a^4 - b^4 - c^4) - 2S(8a^2 + b^2 + c^2) \\ \sqrt{3}(2a^2b^2 - a^2c^2 + 3b^2c^2 - 4b^4 + c^4) + 2S(2a^2 - 2b^2 - c^2) \\ -\sqrt{3}(a^2b^2 - 2a^2c^2 - 3b^2c^2 - b^4 + 4c^4) + 2S(2a^2 - b^2 - 2c^2) \end{bmatrix}$$

Furthermore, side s of the focal equilateral is given by:

$$s^2 = \frac{3}{32}(a^2 + b^2 + c^2 - 2S\sqrt{3}) = \frac{3}{16}(\cot \omega - \sqrt{3})S$$

where ω is the Brocard angle of a triangle, given by $\cot(\omega) = (a^2 + b^2 + c^2)/(2S)$.

Let a_i, b_i, c_i (resp S_i) be the sidelengths (resp. twice the area) of a given triangle \mathcal{T}_i in the grid. Since any \mathcal{T}_i can be used to start the grid:

Corollary 4. *The quantity $a_i^2 + b_i^2 + c_i^2 - 2S_i\sqrt{3}$ is invariant over all \mathcal{T}_i .*

As shown in Figure 16:

Proposition 11. *The axes of the three confocal groups concur at the common X_{16} at 120° angles.*

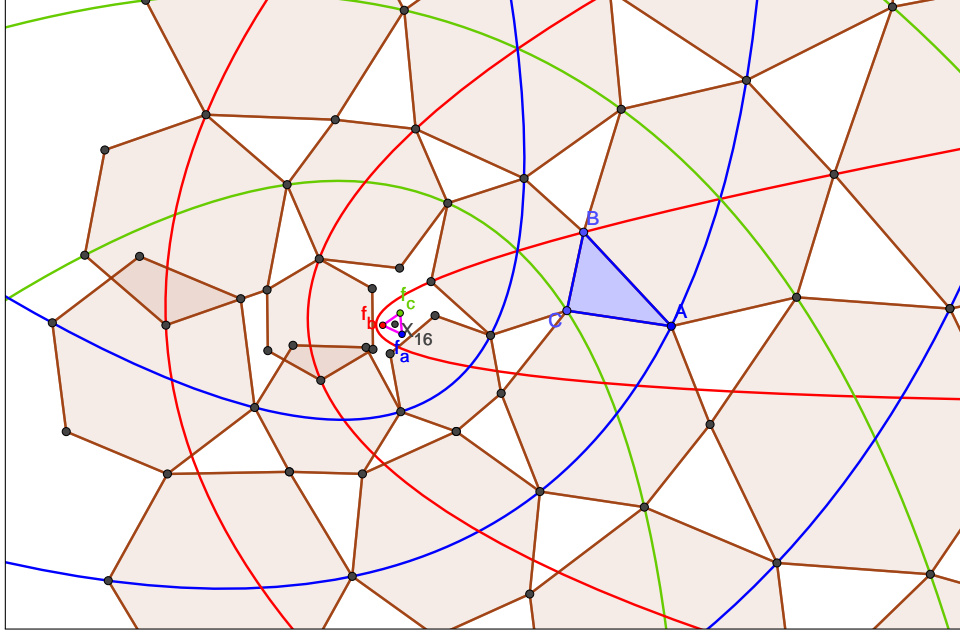


FIGURE 15. Three groups of confocal parabolas (red, green, blue) run along antipodal vertices of hexagons along three 3 major directions. The foci f_a, f_b, f_c of each confocal group are the vertices of an equilateral triangle whose centroid is the X_{16} common to all flank triangles in the grid.

A directrix equilateral. The anticomplement² of the second Fermat point X_{14} is labeled X_{617} on [11].

Proposition 12. *The triangle bounded by the directrices of the A-, B-, and C-parabolas is an equilateral whose centroid is X_{617} , and whose sidelengths s' is given by:*

$$(s')^2 = \left(\frac{S}{4}\right) \left(\frac{5\sqrt{3} + 11 \cot \omega + 16(\sqrt{3} + \cot \omega)}{2 \cos(2\omega) - 1} \right)$$

Note: an expression of the A-vertex of the above appears in [Appendix A](#). Note also that the sidelength is of the directrix equilateral is not conserved across all flank triangles in the grid since each of these will be associated with a different directrix equilateral.

Interestingly, the triangle formed by the vertices of said parabolas is not an equilateral.

Skip-1 confocal parabolas. Let Q_1, A, Q_3, Q_5, \dots (resp. Q_2, B, Q_4, Q_6, \dots) be a sequence of odd (resp. even) side vertices of adjacent hexagons, as shown in [Figure 18](#).

Proposition 13. *The sequence of odd (resp. even) vertices lies on a parabola. The former (resp. latter) is confocal with the A-parabola (resp B-parabola). Furthermore, their axes are parallel to the axis of the C-parabola, and pass through f_b and f_c , respectively.*

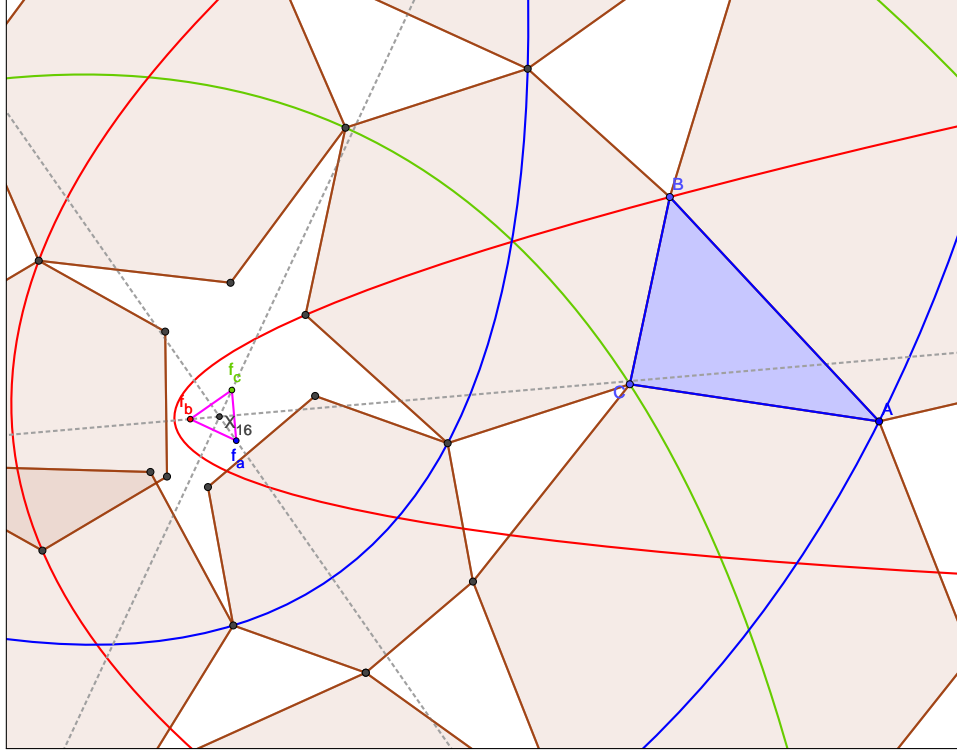


FIGURE 16. Zooming into the focal equilateral f_a, f_b, f_c . Also shown (dashed gray) are the common axes of the 3 confocal parabola groups, all of which pass through the common X_{16} at 120° angles.

The above statements are valid cyclically, i.e., there are families of confocal odd and even parabolas along each of the 3 major directions in the grid, e.g., corresponding to the diagonals of a hexagon erected upon a side of \mathcal{T} .

Computer-usable explicit equations for some of the objects in this section appear in [Appendix A](#).

5. CONTROLLED BY PONCELET

Recall Poncelet's theorem: if a polygon inscribed in one conic simultaneously circumscribes a second one, a 1d family of such polygons exists inscribed/circumscribed about the same conics [5]. In [13] we studied two related families of Poncelet triangles: (i) the homothetic family, and (ii) the Brocard porism, see [Figure 19](#). Geometric details about this family are provided in [Table 1](#).

family	Outer Conic	Inner Conic	Stationary	Conserves
Homothetic	Steiner Ellipse	Steiner Inellipse	X_2	$\sum s_i^2, A, \omega$
Brocard Porism	Circumcircle	Brocard Inellipse	$X_3, X_6, X_{39}, \Omega_1, \Omega_2, X_{15}, X_{16}, \dots$	$\sum s_i^2/A, \omega$

TABLE 1. Geometric details about the homothetic and Brocard porism triangle families.

²This is the double-length reflection about the barycenter X_2 .

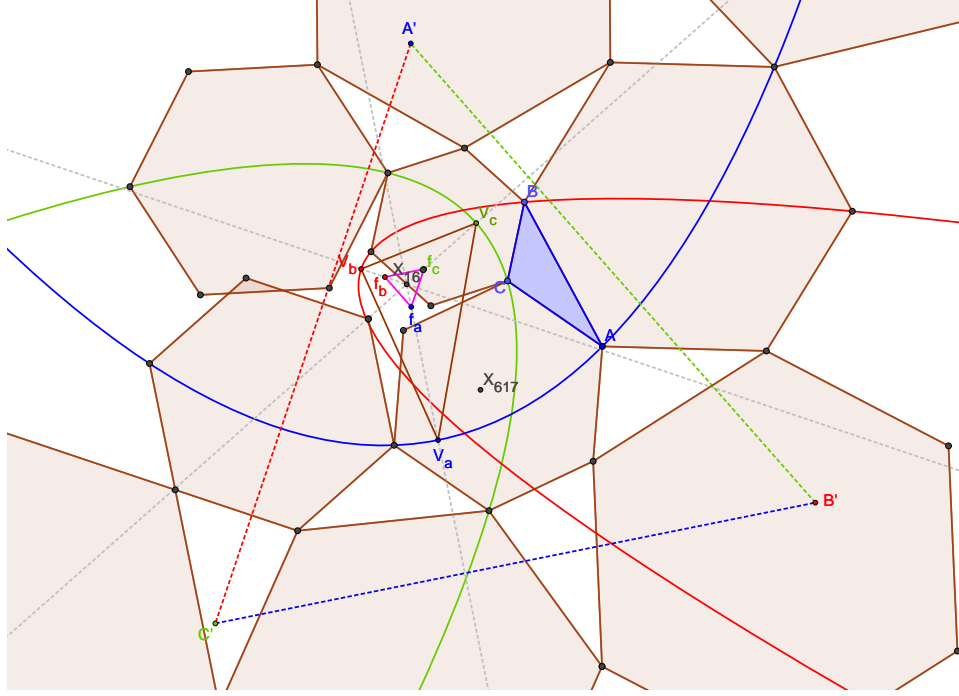


FIGURE 17. The triangle $A'B'C'$ bounded by the directrices (dashed blue, red, and green) of the A -, B -, and C -parabolas (blue, red, red, and green) is also an equilateral, whose centroid is X_{617} . Interestingly, the triangle (brown) connecting the vertices V_a, V_b, V_c of said parabolas is in general a scalene.

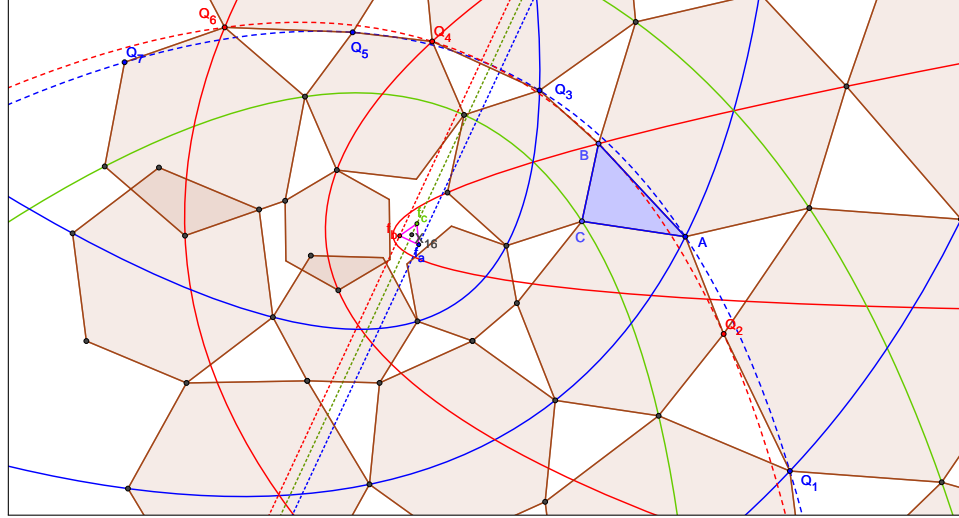


FIGURE 18. Two additional groups of confocal parabolas exist which pass through the odd (resp. even) side vertices along a given grain of the grid. A member of the first (resp. second) confocal group is shown in dashed blue (resp. red), passing through odd vertices $[\dots, Q_1, A, Q_3, Q_5, Q_7, \dots]$ (resp. even vertices) $[\dots, Q_2, B, Q_4, Q_6, \dots]$. The focus of the odd (resp. even) group is f_a (resp. f_b). The major axes of the odd, even, and original C -parabola group are parallel (dashed red, blue, green).

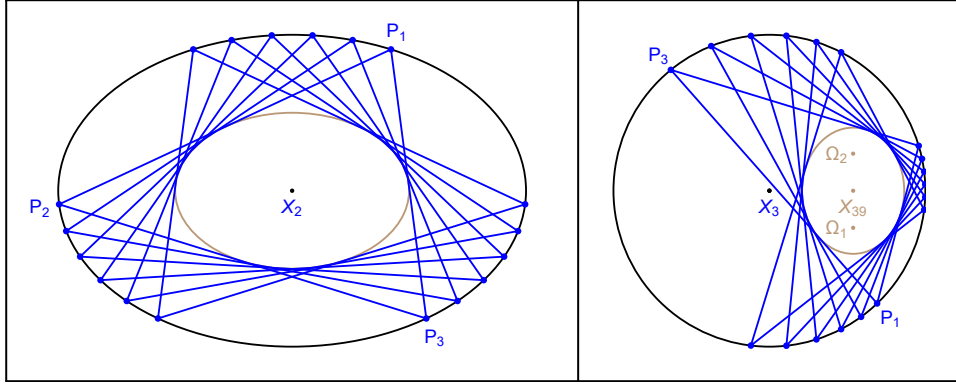


FIGURE 19. **Left:** The “homothetic” family is interscribed between two concentric, homothetic families centered on the fixed barycenter X_2 . **Right:** The Brocard porism are circle-inscribed triangles circumscribing a fixed conic known as the Brocard inellipse, whose foci are the stationary Brocard points Ω_1, Ω_2 of the family.

Homothetic phenomena. Referring to Figure 20, consider our basic construction such that the reference triangle \mathcal{T} is one in the homothetic family.

Referring to the last column of Table 1, notice that the homothetic family conserves both the sum of squared sidelengths and area. Another fact proved in [13] is that the locus of X_k , $k = 13, 14, 15, 16$ over this family are 4 distinct circles.

Since the the side of said equilateral only depends on the sum of squared sidelengths and area Theorem 1:

Corollary 5. *Over homothetic triangle family controlling our grid, the focal equilateral has invariant sidelength and circumradius. Furthermore, the locus of its centroid is a circle concentric with the homothetic pair of ellipses.*

Still referring to Figure 20, experimentally, we observe:

Observation 2. *Over the homothetic family, (i) the locus of the barycenters of the three flanks is an ellipse concentric and axis-aligned with the homothetic pair, though of distinct aspect ratio, and (ii) the locus of the centroids of the three regular hexagons erected on \mathcal{T} is an ellipse which is a 90° -rotated copy of (i).*

Brocard porism phenomena. Referring to Figure 21, consider our basic construction such that the reference triangle \mathcal{T} is one in the Brocard porism.

Let $\mathcal{A} = S/2$ denote the area of a reference triangle. Rewrite the expression for s^2 in Theorem 1 as $s^2 = (3/8)(\cot \omega - \sqrt{3})\mathcal{A}$. Referring to the last column of Table 1, note the Brocard porism conserves ω (though not area), therefore:

Corollary 6. *In a (dynamic) grid controlled by triangles \mathcal{T} in the Brocard porism, the focal equilateral rotates about a fixed centroid X_{16} . Its area is variable and proportional to the area of \mathcal{T} .*

Since X_6 is stationary over the Brocard porism, recalling Proposition 1:

Corollary 7. *Over the Brocard porism, the triangle whose vertices are the X_{15} is perspective with \mathcal{T} at a fixed point (X_6).*

6. VIDEOS & QUESTIONS

Animations illustrating some constructions herein are listed on Table 2.

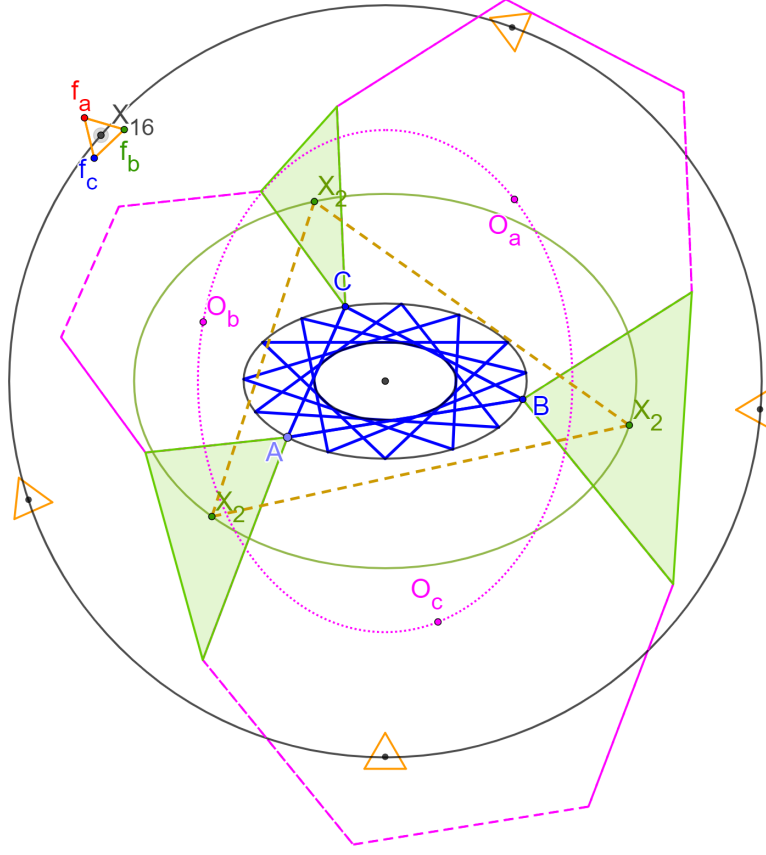


FIGURE 20. Phenomena manifested by objects in our basic construction over homothetic triangles (blue): (i) the focal equilateral (orange) has fixed sidelength and (ii) its centroid moves along a circle (black); (iii) the centroids X_2 of the 3 flank triangles move along a first ellipse (green) concentric with the homothetic pair; (iv) the centroids O_a, O_b, O_c of the three regular hexagons (purple) move along a second ellipse (dotted purple) which is a 90° -rotated copy of (iii).

id	Title	<a href="https://youtu.be/<.>">youtu.be/<.>
01	Basic construction of hexagonal flanks	e3MkijszDEA
02	Circular Loci of X_k , $k = 13, 14, 15, 16$ over the homothetic family	ZwTfwaJJitE

TABLE 2. Videos of some constructions. The last column is clickable and provides the YouTube code.

Open Questions.

- What dynamic properties underlie the fact that certain sequence of hexagonal vertices are spanned by parabolas?
- Does the sequence of hexagons and flank triangles tend to regular shapes away from the foci of the parabolas?
- What are new or different properties of both the basic and grid constructions if hexagons are erected inwardly upon each side of $T = ABC$?
- Depending on the amount of self-intersection (Figure 5) for one or more triangles in the grid, a certain condition is crossed such that the second

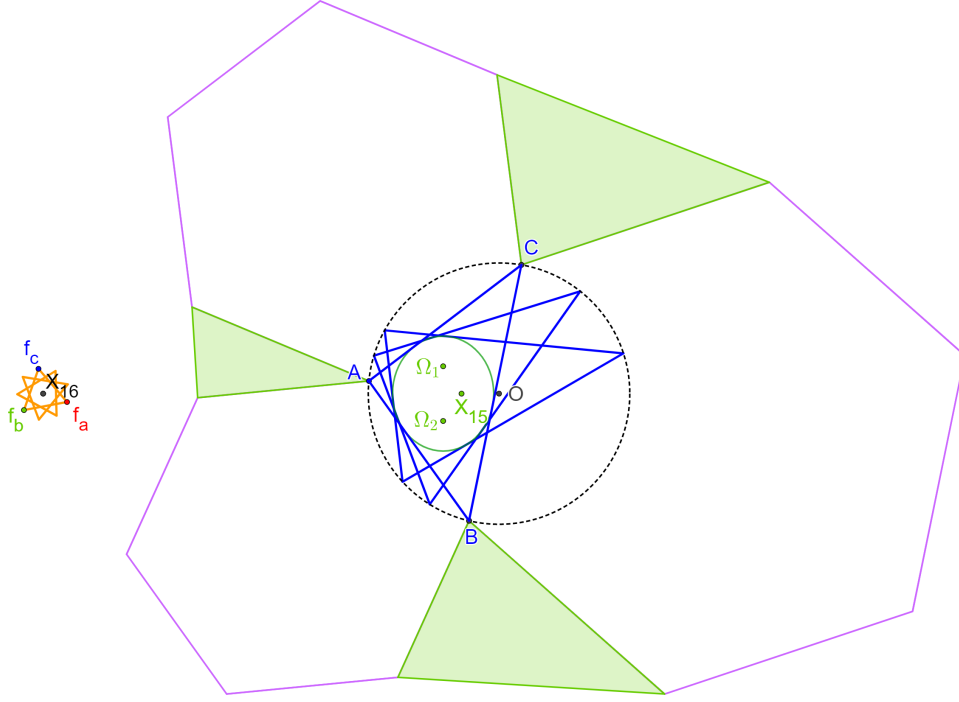


FIGURE 21. The isodynamic points X_{15} and X_{16} of Brocard porism triangles (blue) are stationary isodynamic. This entails that over the porism, flank triangle (green) X_{16} 's will also be stationary. Also shown are corresponding focal equilaterals, whose area is variable and proportional to the area of porism triangles.

isodynamic point wanders away from its fixed common locations. What is that condition? Would using X_{15} be correct?

- Is there an N other than 3, 4, 6 such that interesting properties of similar constructions can be found?
- What happens if self-intersected hexagons are erected, e.g., with vertices common with a simple regular hexagon?

ACKNOWLEDGEMENTS

We thank Arseniy Akopyan for contributing crucial insights and discovering the web of parabolas in the grid. Darij Grinberg lend us an attentive ear and proved the stationarity of X_{16} . Clark Kimberling was kind enough to include our early observations on the Encyclopedia of Triangle Centers.

APPENDIX A. EXPLICIT FORMULAS

To facilitate computational reproduction of our results, we provide code-friendly expressions for a few objects. In the expressions below a, b, c refer to sidelengths and x, y, z are barycentric coordinates.

A.1. A-parabola. It is given implicitly by:

$$2*(a^8-4*a^6*b^2+6*a^4*b^4-4*a^2*b^6+b^8-4*a^6*c^2+13*a^4*b^2*c^2-14*a^2*b^4*c^2+5*b^6*c^2+6*a^4*c^4-23*a^2*b^2*c^4+15*b^4*c^4-4*a^2*c^6+$$

$$\begin{aligned}
& 14b^2c^6+c^8)xy-3c^2(2a^6-8a^4b^2+ \\
& 10a^2b^4-4b^6-5a^4c^2+18a^2b^2c^2- \\
& 11b^4c^2+4a^2c^4-8b^2c^4-c^6) y^2+2(a^8-4a^6b^2+ \\
& 6a^4b^4-4a^2b^6+b^8-4a^6c^2+13a^4b^2c^2- \\
& 23a^2b^4c^2+14b^6c^2+6a^4c^4-14a^2b^2c^4+ \\
& 15b^4c^4-4a^2c^6+5b^2c^6+c^8) xz+2(4a^8- \\
& 13a^6b^2+15a^4b^4-7a^2b^6+b^8-13a^6c^2+ \\
& 31a^4b^2c^2-35a^2b^4c^2+17b^6c^2+15a^4c^4- \\
& 35a^2b^2c^4+36b^4c^4-7a^2c^6+17b^2c^6+c^8) yz- \\
& 3b^2(2a^6-5a^4b^2+4a^2b^4-b^6-8a^4c^2+ \\
& 18a^2b^2c^2-8b^4c^2+10a^2c^4-11b^2c^4-4c^6) z^2+ \\
& 2\sqrt{3}S(2(a^6-3a^4b^2+3a^2b^4-b^6-5a^4c^2+ \\
& 9a^2b^2c^2-4b^4c^2+7a^2c^4-7b^2c^4-3c^6) xy+ \\
& (a^2-b^2-c^2)(2a^4-4a^2b^2+2b^4-10a^2c^2+ \\
& 8b^2c^2+5c^4) y^2+2(a^6-5a^4b^2+7a^2b^4-3b^6- \\
& 3a^4c^2+9a^2b^2c^2-7b^4c^2+3a^2c^4-4b^2c^4-c^6) xz+ \\
& 2(2a^6-7a^4b^2+8a^2b^4-3b^6-7a^4c^2+17a^2b^2c^2- \\
& 12b^4c^2+8a^2c^4-12b^2c^4-3c^6) yz+(a^2-b^2-c^2)(2a^4- \\
& 10a^2b^2+5b^4-4a^2c^2+8b^2c^2+2c^4) z^2)=0
\end{aligned}$$

The B - and C -parabolas can be obtained by cyclic permutations, i.e., $(a, b, c) \rightarrow (b, c, a)$, and $(a, b, c) \rightarrow (c, a, b)$, respectively.

A.2. The two “skip-1” parabolas. The skip-1 parabola through B is given by:

$$\begin{aligned}
& (\sqrt{3}(2a^6 - 5a^4b^2 + 4a^2b^4 - b^6 - 7a^2b^2c^2 + \\
& 3b^4c^2 - 3a^2c^4 + 3b^2c^4 + c^6) + 6(6a^4 - 5a^2b^2 + \\
& b^4 - 4a^2c^2 + 2b^2c^2 + c^4)S) x^2 + (\sqrt{3}(3a^6 - \\
& 7a^4b^2 + 5a^2b^4 - b^6 + 6a^4c^2 - 10a^2b^2c^2 + \\
& 2b^4c^2 - 3a^2c^4 + 5b^2c^4) + 2(13a^4 - 8a^2b^2 + \\
& b^4 - 17a^2c^2 + 7b^2c^2 + 4c^4)S) xy + (\sqrt{3}(4a^6 - \\
& 14a^4b^2 + 13a^2b^4 - 3b^6 - 4a^4c^2 - 13a^2b^2c^2 + \\
& 4b^4c^2 - a^2c^4 + 4b^2c^4 + c^6) + 2(22a^4 - 14a^2b^2 + \\
& b^4 - 8a^2c^2 + 7b^2c^2 + c^4)S) xz + (\sqrt{3}(5a^6 - \\
& 7a^4b^2 + 2a^2b^4 + 6a^4c^2 + 3a^2b^2c^2 - 2b^4c^2 - \\
& 6a^2c^4 + b^2c^4 + c^6) - 2(11a^4 - 10a^2b^2 + 2b^4 - \\
& a^2c^2 + 2b^2c^2 - c^4)S) yz + (\sqrt{3}(a^6 - 15a^4b^2 + \\
& 9a^2b^4 - b^6 - 2a^4c^2 - 3a^2b^2c^2 - b^4c^2 + a^2c^4 + \\
& 2b^2c^4) + 6(3a^4 + 2a^2b^2 - b^4 - a^2c^2)S) z^2 = 0
\end{aligned}$$

The skip-1 parabola through C is obtained with a bicentric substitution, i.e., $(a, b, c, x, y, z) \rightarrow (a, c, b, x, z, y)$.

A.3. Center (at infinity) of the A-parabola group. The A -parabola and BC skip-1 pair of parabolas have parallel axes through f_a, f_b, f_c , therefore their axes will cross the line at infinity at the same point given by the following barycentrics;

$$x=8a^6 - 8a^4b^2 + a^2b^4 - b^6 - 8a^4c^2 + 6a^2b^2c^2 + b^4c^2 + a^2c^4 + b^2c^4 - c^6 + 2\sqrt{3}(b^2 - c^2)^2S$$

$$\begin{aligned}
y=& -4a^6 + a^4b^2 + a^2b^4 + 2b^6 + 7a^4c^2 - 3a^2b^2c^2 - \\
& 5b^4c^2 - 2a^2c^4 + 4b^2c^4 - c^6 - 2\sqrt{3}(a^2 - \\
& c^2)(b^2 - c^2)S
\end{aligned}$$

$$z = -4a^6 + 7a^4b^2 - 2a^2b^4 - b^6 + a^4c^2 - 3a^2b^2c^2 + 4b^4c^2 + a^2c^4 - 5b^2c^4 + 2c^6 + 2\sqrt{3}(a^2 - b^2)(b^2 - c^2)S$$

A.4. **Directrix of the A-parabola.** Is is the line given by:

$$(a^4 - 8a^2b^2 + 12b^4 - 8a^2c^2 + 27b^2c^2 + 12c^4 - 2\sqrt{3}(2a^2 - 5b^2 - 5c^2)S)x + (6a^4 - 23a^2b^2 + 22b^4 - 30a^2c^2 + 58b^2c^2 + 39c^4 + 2\sqrt{3}(a^2 - 3b^2 - 2c^2)S)y + (6a^4 - 30a^2b^2 + 39b^4 - 23a^2c^2 + 58b^2c^2 + 22c^4 + 2\sqrt{3}(a^2 - 2b^2 - 3c^2)S)z = 0$$

The other two directrices can be obtained via cyclic substitution.

A.5. **Directrix equilateral.** The barycentrics x, y, z of the A -vertex of the directrix equilateral (Proposition 12) are given by:

$$x = -\sqrt{3}(12a^6 - 13a^4b^2 - a^2b^4 + 2b^6 - 13a^4c^2 - 8a^2b^2c^2 - 2b^4c^2 - a^2c^4 - 2b^2c^4 + 2c^6) - 6(3a^2b^2 + 3a^2c^2 + 2b^2c^2)S;$$

$$y = \sqrt{3}(5a^6 + 2a^4b^2 - 10a^2b^4 + 3b^6 - 7a^4c^2 - 10a^2b^2c^2 - a^2c^4 - 6b^2c^4 + 3c^6) - 6(a^4 - 5a^2b^2 + b^4 - 3b^2c^2 - c^4)S;$$

$$z = \sqrt{3}(5a^6 - 7a^4b^2 - a^2b^4 + 3b^6 + 2a^4c^2 - 10a^2b^2c^2 - 6b^4c^2 - 10a^2c^4 + 3c^6) - 6(a^4 - b^4 - 5a^2c^2 - 3b^2c^2 + c^4)S.$$

REFERENCES

- [1] Akopyan, A. (2021). Private communication. 6, 8, 9
- [2] Čerin, Z. (1998). Regular hexagons associated to triangles with equal centroids. *Elem. Math.*, 53: 112–118. 2
- [3] Čerin, Z. (2002). Loci related to variable flanks. *Forum Geometricorum*, 2: 105–113. 2
- [4] Dosa, T. (2007). Some triangle centers associated with the excircles. *Forum Geometricorum*, 7: 151–158. 2
- [5] Dragović, V., Radnović, M. (2011). *Poncelet Porisms and Beyond: Integrable Billiards, Hyperelliptic Jacobians and Pencils of Quadrics*. Frontiers in Mathematics. Basel: Springer. books.google.com.br/books?id=QcOmDAEACAAJ. 13
- [6] Fukuta, J. (1996). Problem 10514. *Amer. Math. Monthly*, 103. Solution: vol. 104 (1997), p.775. 2
- [7] Fukuta, J. (1996). Problem 1493. *Math. Mag.*, 69. Solution: 70 (1997), pp.70–73. 2
- [8] Grinberg, D. (2021). Private communication. 4
- [9] Hoehn, L. (2001). Extriangles and excevians. *Math. Magazine*, 74: 384–388. 2
- [10] Johnson, R. (1917). Directed angles and inversion with a proof of Schoute’s theorem. *Am. Math. Monthly*, 24: 313–317. 3
- [11] Kimberling, C. (2019). Encyclopedia of triangle centers. faculty.evansville.edu/ck6/encyclopedia/ETC.html. 3, 12
- [12] van Lamoen, F. (2001). Friendship among triangle centers. *Forum Geometricorum*, 1: 1–6. 1, 2
- [13] Reznik, D., Garcia, R. (2021). Related by similarity II: Poncelet 3-periodics in the homothetic pair and the Brocard porism. *Intl. J. Geom.*, 10(4): 18–31. 13, 15
- [14] Stachel, H. (2002). Napoleon’s theorem and generalizations through linear maps. *Beiträge zur Algebra und Geometrie*, 43(2): 433–444. 2

- [15] Weisstein, E. (2019). Mathworld. *MathWorld—A Wolfram Web Resource*. mathworld.wolfram.com. 1, 2, 3, 4, 8